

WEATHERING OF SOILS IN ALPINE AREAS AS INFLUENCED BY CLIMATE AND PARENT MATERIAL

MARKUS EGLI^{1,*}, ALDO MIRABELLA², ALESSANDRO MANCABELLI³ AND GIACOMO SARTORI⁴

¹ Department of Geography, University of Zürich, Winterthurerstrasse 190, 8057 Zürich, Switzerland

² Istituto Sperimentale per lo Studio e la Difesa del Suolo, Piazza D'Azeglio 30, 50121 Firenze, Italy

³ Istituto Tecnico Agrario, Via Edmondo Mach 1, 38010 S. Michele all'Adige-Trento, Italy

⁴ Museo Tridentino di Scienze Naturali, Via Calepina 14, 38100 Trento, Italy

Abstract—Two soil sequences in northern Italy (Val di Fiemme and Val Genova) along an elevational gradient ranging from moderate (950 m a.s.l.) to high alpine (2440 m a.s.l.) climate zones were investigated with respect to element losses (Ca, Mg, K, Na, Fe, Al, Si, Mn) and development of clay minerals. Soils formed on paleo-rhyolitic parent material in Val di Fiemme and on tonalitic-granodioritic morainic material in Val Genova. All the soils have a similar age (~12,000 y) and have been classified as Podzols. The soils are very acid and the pH values tend to increase with decreasing altitude. Podzolization processes were most intense in the range of the subalpine forest up to the timberline (1400–1900 m above sea-level (a.s.l.)). Element leaching was greatest in this range and weathering rates decrease with both higher and lower altitudes. Due to the different lithologies and precipitations between the two valleys, the total amount of chemical weathering was slightly different, although the same trends with altitude could be observed. Imogolite-type materials (ITM) are generally of minor importance. Greater concentrations of ITM were observed in the Bhs or Bs horizons of the Episkeleti-Entic Podzols at the lower altitudes. Iron eluviation was similar in all Podzols while larger amounts of eluviated Al were detected in Val Genova. The pattern of smectite distribution along the climosequences had similarities to the trend of cation losses. The largest amount of low-charge expandable minerals seems to exist in the range of the subalpine forest up to the timberline. The development of clay minerals with a smaller layer charge was more advanced in Podzols on rhyolitic material where smectite could be detected in the Bhs and Bs horizon. Parent material influenced chemical weathering in the soils along the two climosequences and essentially determined the degree of weathering and the formation of clay minerals.

Key Words—Alps, Climosequence, Parent Material, Podzol, Smectite, Weathering.

INTRODUCTION

The quantification of silicate weathering rates and the identification of clay mineral formation processes have important implications for a diverse range of geochemical issues, amongst which are rates of neutralization of acids via silicate hydrolysis reaction and the link between weathering rates and the long-term control on atmospheric CO₂ (Berner and Lasaga, 1989).

Although almost negligible on a worldwide scale, the Alps and their soils are an essential element of the landscape of Central Europe. Several studies have been carried out in recent years on soils developing in Alpine environments of north-eastern Italy and southern Switzerland. These studies have elucidated the chemical and mineralogical processes leading to the formation of Podzols. In particular, the influence of three soil-forming factors, climate, time and parent material have been taken into account (Mirabella and Sartori, 1998; Righi *et al.*, 1999; Egli *et al.*, 2001a, 2001b, 2003; Mirabella *et al.*, 2002).

Weathering rates of individual soils differ due to varying soil properties and surrounding environmental conditions. Soil sequences may give insight into the influence of individual factors on the weathering rates. Jenny (1980) differentiates the following sequences: lithosequences (differences in parent mineralogy), climosequences (differences in precipitation and/or temperature), toposequences (lateral variations in slope and topography), chronosequences (effect of time on chemical weathering), and biosequences (variation in biota and its influence on chemical weathering).

Despite the efforts made at investigating the mechanisms involved in the podzolization and weathering processes, greater understanding of the mineral-reaction pathways as a function of climate and parent material is necessary. Minor mineralogical variations in the parent material may lead to differing weathering pathways and, therefore, end-products. Recent works on Podzols and associated Dystrochrepts in European Alpine environments reported the presence of smectite components in surface horizons (Righi and Meunier, 1991; Righi *et al.*, 1993; Carnicelli *et al.*, 1997; Mirabella and Sartori, 1998). The formation of smectite-like compounds in the E horizon during pedogenesis, for instance, requires a corresponding minimal amount of chlorite and/or tri-

* E-mail address of corresponding author:
megli@geo.unizh.ch

DOI: 10.1346/CCMN.2004.0520304

octahedral (and dioctahedral) mica. If almost no other 2:1 mineral components are present in the silicate parent material, then a micaceous (muscovite-like) mineral component can become the dominant end-product of clay-mineral weathering (Mirabella *et al.*, 2002).

Climate is of growing interest with respect to landscape and consequently to soil evolution because of worldwide climate changes. Climate warming due to anthropogenic emissions of greenhouse gases is predicted to increase the Earth's average surface temperature during the next 50–100 y. Earlier studies documented the effect of differences in climate along an elevational gradient, generally a decrease in temperature and an increase in precipitation, on plant communities and soil taxa. Common trends reported in these studies included changes in soil organic matter, soil acidity, and exchangeable ions (e.g. Whittaker *et al.*, 1986; Mahaney, 1978; Bockheim *et al.*, 2000). The relationship between climate and element weathering is strongly non-linear and is thought to be overshadowed by the pronounced podzolization effect near the timberline in Alpine areas. Greater precipitation rates and the production of chelating compounds in the soil are believed to promote the appearance of smectites (Egli *et al.*, 2003) that seem to be the end-product of weathering in such areas.

The present work focuses on element weathering and clay mineral transformations along a climosequence in an Alpine area of northern Italy. The new results could be compared to a previous climosequence study of soils developing on a different lithology in a nearby region.

INVESTIGATION AREA

A sequence of four soil profiles in the Val di Fiemme (northern Italy; Figure 1) along an elevational gradient ranging from 960 up to 2050 m a.s.l. was investigated (Table 1). The soil profiles were selected during a soil cartographic inventory and are assumed to be representative of the elevational zones. The soils were transitions from Episkeleti-Eentic to Endoskeletal Podzols (Tables 1 and 2). All the soils developed on (paleo-)rhyolite. The climate ranges from temperate to subalpine (near the timberline).

This sequence could be compared to another one in the nearby Val Genova, with a similar climate range (from 950 up to 2440 m a.s.l.) and tonalitic or granodioritic parent material. The soils in the Val Genova varied from Umbric Leptosols to Haplic Podzols (Egli *et al.*, 2003). Compared to the Val Genova, the climatic conditions in Val di Fiemme are a little drier (850 mm precipitation per year at 960 m a.s.l. up to ~1400 mm at 2050 m a.s.l.; Costantini *et al.* (1995) and Servizio Idrografico (1959)) against Val Genova with 1190 mm at 950 m a.s.l. and ~1800 mm at 2100 m a.s.l. (Egli *et al.*, 2003). The annual temperature varies in Val di Fiemme from 7.9°C at 950 m a.s.l. to ~2°C at 2050 m a.s.l.

MATERIAL AND METHODS

Soil sampling

Approximately 4–5 kg of soil material were collected per soil horizon from excavated profile pits. In

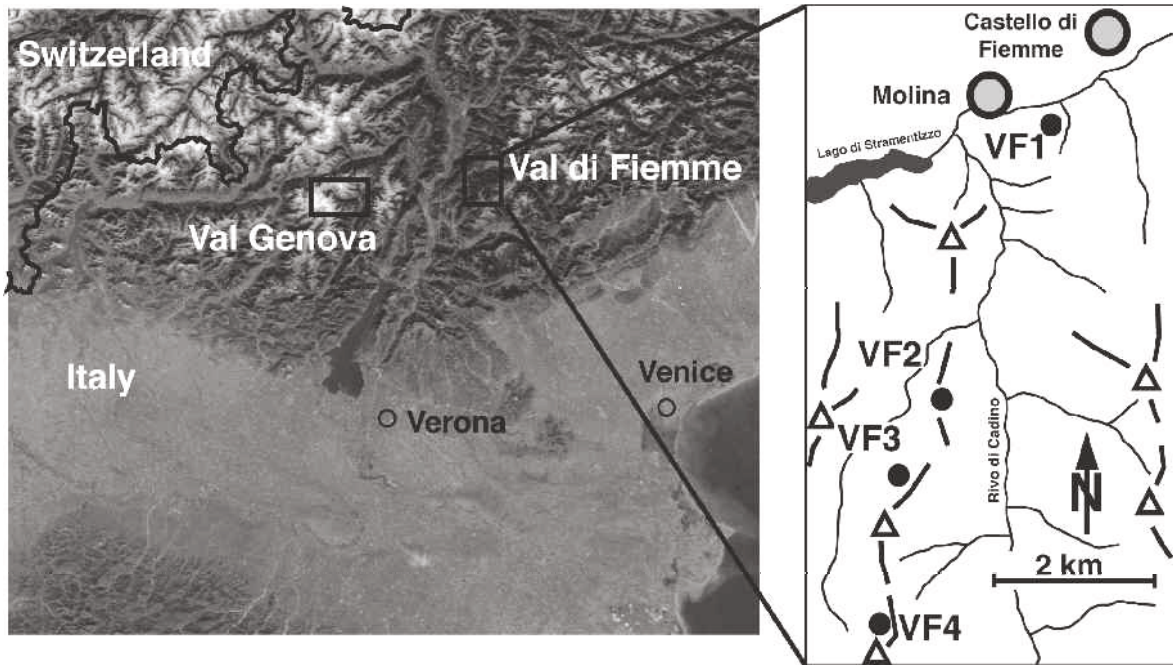


Figure 1. Location of the study area Val di Fiemme (data source: satellite image 'Terra'; Jacques Descloitres, MODIS Land Rapid Response Team, NASA/GSFC), of the investigation sites VF1–4 and the nearby Val Genova.

Table 1. Characteristics of the study sites in Val di Fiemme, Southern Alps.

Profile	Location	Elevation (m a.s.l.)	Aspect (°N)	Slope (%)	Parent material	Vegetation	WRB (1998)
VF1	Madonna dei Boscaioli	960	15	60	(Paleo) rhyolite-debris	<i>Abietetum</i>	Episkeleti-Entic Podzol
VF2	Baito di Costa Canton	1425	360	60	(Paleo) rhyolite, morainic material	<i>Abietetum</i>	Episkeleti-Entic Podzol
VF3	Villa di Catarinella	1705	340	45	(Paleo) rhyolite-debris	<i>Piceetum</i>	Endoskeletal-Densic Podzol
VF4	Monte Brustelon	2050	360	35	(Paleo) rhyolite-debris	<i>Larici-Piceetum</i>	Endoskeletal Podzol

order to yield reasonable results, large soil-sampling volumes are needed for soils in alpine areas (Hitz *et al.*, 2002). Soil bulk density was determined by a soil core sampler (or by excavated holes with a volume of 500–2000 mL that were backfilled with a measurable volume of quartz sand). Taking advantage of the profile pits, undisturbed soil samples down to the C horizon were extracted.

Soil chemistry

Element pools in the soil (Ca, Mg, K, Na, Fe, Al, Mn, Si, Ti and V) were determined by a method of total dissolution. Oven-dried (70°C, over 48 h) samples were dissolved using a mixture of HF, HCl, HNO₃ and H₃BO₃ as in Fitze *et al.* (2000). Concentrations of Ca, Mg, K, Na, Fe, Mn, Al, Si, Ti and V were determined by atomic absorption spectroscopy, in part using a graphite furnace

(V). Additionally, the dithionite- and oxalate-extractable fraction was measured for the elements Fe, Al and Si (McKeague *et al.*, 1971). Total C and N contents of the soil were measured with a C/H/N analyzer (Elementar Vario EL). Soil pH (in 0.01 M CaCl₂) was determined on air-dried samples of fine earth using a soil:solution ratio of 1:2.5.

Soil mineralogy

The clay fraction (<2 µm) was obtained from the soil after destruction of organic matter with dilute and Na acetate-buffered H₂O₂ (pH 5) by dispersion with Calgon and sedimentation in water (Carnicelli *et al.*, 1997). Oriented specimens on glass slides were analyzed by X-ray diffraction (XRD) using CuKα radiation from 2 to 15°2θ with steps of 0.02°2θ at 2 s per step. The following treatments were performed: Mg saturation,

Table 2. Characteristic properties of the soils investigated at Val di Fiemme.

Site	Soil depth (cm) and soil type	Soil horizon	Munsell color moist	Bulk density (g cm ⁻³)	Sand ¹ (%)	Silt (%)	Clay (%)
VF1	Episkeleti-Entic Podzol	0–20	AE	5YR 2.5/2	1.06	40	45
		20–50	Bs1	5YR 4/4	1.34	53	40
		50–90	Bs2	5YR 4/6	1.36	51	44
		>90	C	7.5YR 4/3	1.58	60	36
VF2	Episkeleti-Entic Podzol	0–20	AE	2.5YR 4/1	0.97	51	37
		20–60	Bs1	2.5YR 3.5/6	1.03	75	21
		60–120	Bs2	5YR 4/4	1.28	73	24
		120–145	BC(m)	5YR 4/6	88	10	2
		>145	C	7.5YR 5/4	1.49	66	32
VF3	Endoskeletal-Densic Podzol	0–20	E	7.5YR 5/2	0.74	43	46
		20–28	Bhs	2.5YR 3/2	0.75	24	57
		28–60	Bs	7.5YR 4/5	1.03	45	45
		>60	BC (m)	10YR 4/2	1.53	61	30
VF4	Endoskeletal Podzol	0–20	E	5YR 4/2	0.95	47	40
		20–38	Bs1	7.5YR 4/4	0.93	34	54
		38–60	Bs2	2.5YR 3/2	45	44	10
		>60	C	2.5YR 4/4	1.53	65	33

¹ Size fractions: sand = 2000–50 µm, silt = 50–2 µm, clay = <2 µm

ethylene-glycol solvation (EG) and K saturation, followed by heating for 2 h at 335 and 550°C. Prior to these treatments, amorphous Al and Fe phases were dissolved using an oxalate extraction in samples from the Bs and BC horizons of all soils and from the surface horizon of VF4. Randomly oriented powder mounts were prepared by filling glass holders and were step-scanned from 58 to 64°2θ with steps of 0.02°2θ at 10 s per step.

Digitized XRD data were routinely smoothed and corrected for Lorentz and polarization factors (Moore and Reynolds, 1997). Peak separation and profile analysis were carried out by the Origin PFM® using the Pearson VII algorithm after smoothing the diffraction patterns by a Fourier transform function. Background values were calculated by means of a non-linear function (polynomial 2nd order function; Lanson, 1997). Layer-charge estimation of clays was performed using the long-chain alkylammonium ion C18 according to the method proposed by Olis *et al.* (1990).

For the monolayer to bilayer transition, the following equation was used:

$$d_{001} = 8.21 + 34.22 \text{MLC} \quad (1)$$

with MLC = mean layer charge and d values given in Å.

For the bilayer to pseudotrimolecular layer transition, the equation is:

$$d_{001} = 8.71 + 29.65 \text{MLC} \quad (2)$$

The presence of kaolinite was checked using conventional infrared (IR) spectra of soil clay.

'Imogolite-type material' (ITM), henceforth meaning the sum of imogolite and proto-imogolite allophane, was estimated (assuming that the Al/Si molar ratio is close to 2.0) according to Parfitt and Henmi (1982), *i.e.* as allophane + imogolite% = Si(oxalate)% × 7.1.

The main mineralogy of the bulk material (skeleton and fine earth) was determined optically and by normative calculations.

Calculation of weathering rates

The weathering rates of soils were derived from calculations of enrichment/depletion factors determined using immobile element contents. The derivation of mass-balance equations and their applications to pedologic processes were discussed in detail by Brimhall and Dietrich (1987) and Chadwick *et al.* (1990) and revised by Egli and Fitze (2000). Volumetric changes that occur during pedogenesis were determined by adopting the classical definition of strain, $\varepsilon_{i,w}$ (Brimhall and Dietrich, 1987):

$$\varepsilon_{i,w} = \frac{\Delta z_w}{\Delta z} - 1 \quad (3)$$

with Δz as the columnar height (m) of a representative elementary volume of protore (or unweathered parent material) ' p ' and Δz_w is the weathered equivalent height (m) ' w '. The calculation of the open-system mass

transport function $\tau_{j,w}$ is defined by (Chadwick *et al.*, 1990)

$$\tau_{j,w} = \left(\frac{\rho_w C_{j,w}}{\rho_p C_{j,p}} (\varepsilon_{i,w} + 1) \right) - 1 \quad (4)$$

with $C_{j,p}$ (kg/t) as the concentration of element j in the protolith (*e.g.* unweathered parent material, bedrock), $C_{j,w}$ as the concentration of element j in the weathered product (kg/t), and with ρ_p and ρ_w being the bulk density (t/m³) of the protolith and weathered soil, respectively.

With n soil layers, the calculation of changes in mass of element j is given by (Egli and Fitze, 2000)

$$\bar{m}_{j,\text{flux}(z_w)} = \sum_{a=1}^n C_{j,p} \rho_p \left(\frac{1}{\varepsilon_{i,w} + 1} \right) \tau_{j,w} \Delta z_w \quad (5)$$

where $\tau_{j,w}$ corresponds to the mass transport function, $\varepsilon_{i,w}$ to the strain and Δz to the weathered equivalent of the columnar height (m) of a representative elementary volume.

Two important assumptions concerning elemental components are required in the mass balance calculations using immobile elements (White and Blum, 1995). The first involves the determination of the composition of the parent material. For soils developed in sites on bedrock, the potential errors are confined to local heterogeneities in bedrock composition. The estimate of the initial composition becomes more difficult when soils are developed on sedimentary parent materials such as alluvial terraces, loess deposits, debris or morainic material. For such deposits, the least weathered horizon in the soil profile is assumed to be the parent material. The second requirement is that weatherable elements must be ratioed against an inert component i , present in both the parent material and the soil. Ti, Zr or V are often considered to be almost immobile.

RESULTS

Soil chemistry

All soils of the investigation area, Val di Fiemme, had a sandy to silty-sandy texture. Due to the granitic geochemistry of the parent material (paleo-thylolite), the acidification of the soils is pronounced. Eluviation and illuviation of Fe and Al is typical for all soils. The Podzols of the sites VF3 and VF4 show, furthermore, a translocation of soil organic matter (SOM).

Some smaller amounts of ITM were observed in the Bhs and Bs horizons of the Podzols at the sites VF3 and VF4 and to a greater extent in the Bs horizons of the Episkeleti-Entic Podzols (Table 3). The ITM is reported to be a common soil constituent in Bs horizons of Podzols or Podzol-like soils worldwide (Lumsdon and Farmer, 1997) and must have been formed by reaction in solution between inorganic Al cations and orthosilicic acid when the solubility product for these minerals was

Table 3. Chemical properties of the fine earth (<2 mm) of the investigated soils from Val di Fiemme.

Site	Soil horizon	pH (CaCl ₂)	Org. C (%)	N (%)	Al _d ¹ (%)	Fe _d (%)	Al _o ² (%)	Fe _o (%)	ITM ³ (%)
VF1	AE	4.7	6.32	0.309	0.32	1.08	0.34	0.28	0.23
	Bs1	4.5	2.43	0.111	0.62	1.14	0.94	0.35	1.88
	Bs2	4.8	1.51	0.058	0.54	1.14	1.04	0.48	2.59
	C	4.5	0.37	0.004	0.16	0.86	0.20	0.12	0.28
VF2	AE	3.2	5.82	0.253	0.16	0.85	0.15	0.11	0.01
	Bs1	4.5	3.24	0.112	0.97	0.96	1.44	0.54	2.83
	Bs2	4.7	0.60	0.011	0.41	0.64	0.70	0.22	1.69
	BCm	4.9	0.40	0.005	0.31	0.51	0.43	0.09	1.18
	C	4.7	0.28	0.017	0.22	0.61	0.31	0.08	0.69
VF3	E	3.0	4.86	0.223	0.1	0.59	0.12	0.07	0.01
	Bhs	3.5	11.56	0.444	1.22	2.62	1.13	1.86	0.20
	Bs	3.9	7.49	0.249	1.58	1.93	1.64	1.35	0.60
	BC (m)	3.9	7.83	0.237	1.46	1.61	1.53	0.93	0.32
VF4	E	3.5	3.68	0.148	0.15	0.7	0.13	0.15	0.01
	Bs1	3.8	4.51	0.160	0.72	1.17	0.70	0.93	0.04
	Bs2	4.1	8.86	0.314	2.53	2.32	2.57	1.50	0.47
	C	4.4	0.95	0.010	0.46	0.99	0.45	0.12	0.44

¹ dithionite extractable fraction² oxalate extractable fraction³ ITM: imogolite-type material

exceeded. Allophanic precipitates are found in Bs horizons with pH values which are not too low unless Al is preferentially trapped in vermiculitic interlayers (Lumsdon and Farmer, 1997). The low pH in the Bs or Bhs horizons of the Podzols at the sites VF3 and VF4 must therefore have inhibited the formation of a greater amount of ITM.

Due to the good correlation between Al_d or Al_o (and partially Fe_o) and Si_o at sites VF1 and VF2, translocation of dissolved Al and Si from the weathering of minerals in the topsoil seems to be likely (Figure 2). Al and partially also Fe seem to be translocated into the B horizon as proto-imogolite sol. Incongruent weathering within the B horizons of these soils as a source of ITM production (Gustafsson *et al.*, 1995) cannot, however, be excluded. Due to the accumulation of organic C in the subsoil, the translocation of Al and Fe in the two other soils seems primarily to be promoted by chelating organic matter.

The parent materials have uniform geochemical compositions. The SiO₂ content (Table 4) in the C horizons is close to 70%. This reflects the siliceous, rhyolitic character of the parent material. The distribution of SiO₂ (if the SiO₂ content is referred to as 'humus-free' material and the component sum is kept to 100%) through the soil profile shows an enrichment of SiO₂ in the AE or E horizon (with 72.3% in the AE of VF1; 78.2% in the AE of VF2; 80.1% in the E of VF3; and 77.1% in the E of VF4). Compared to the Val Genova

site, the parent material has lower Ca but higher Mg and K contents (*cf.* Egli *et al.*, 2003; see also 'Discussion and conclusions').

Chemical weathering

Losses or gains of an element during pedogenesis are calculated using equation 1. For calculations based on inert standards like Ti or V that have been used in this investigation, one of the prerequisites is the homogeneity of the parent material which cannot be taken for granted in all cases. The best strategy is to use a suite of immobile elements. The calculation with V gave unrealistic high or low element losses and, thus, indicates fractionation rather than weathering processes.

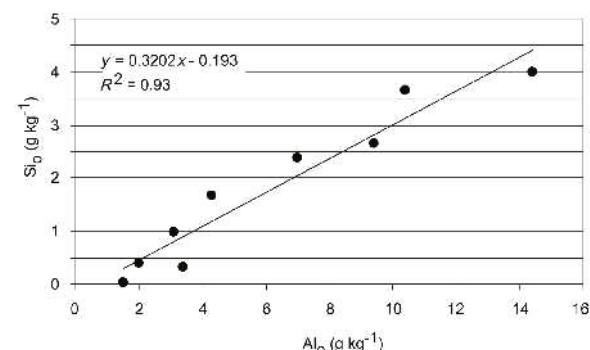


Figure 2. Relationship between the oxalate-extractable Al and Si in the soils VF1 and VF2 at the investigation site Val di Fiemme.

Table 4. Geochemical characteristics (total analysis of the bulk material including soil skeleton (>2 mm up to 200 mm) and fine earth (<2 mm)) of the soils of Val di Fiemme.

Site and soil horizon	Depth (cm)	Org. matter ¹ (g kg ⁻¹)	Al ₂ O ₃ (g kg ⁻¹)	SiO ₂ (g kg ⁻¹)	TiO ₂ (g kg ⁻¹)	CaO (g kg ⁻¹)	MgO (g kg ⁻¹)	K ₂ O (g kg ⁻¹)	Na ₂ O (g kg ⁻¹)	Fe ₂ O ₃ (g kg ⁻¹)	MnO ₂ (g kg ⁻¹)	VOOH (g kg ⁻¹)	Σ (g kg ⁻¹)
VF1													
AE	0–20	66	125	639	5.7	3.4	20	43	22	26	0.45	0.045	950
Bs1	20–50	22	132	676	5.8	1.9	23	47	23	26	0.38	0.044	956
Bs2	50–90	9	146	696	7.0	2.4	33	46	25	29	0.42	0.056	993
C	> 90	2	137	716	6.2	2.7	33	49	26	25	0.40	0.042	997
VF2													
AE	0–20	72	98	703	5.7	2.1	17	37	17	20	0.15	0.048	970
Bs1	20–60	40	136	645	4.7	3.0	26	41	21	25	0.18	0.040	940
Bs2	60–120	7	135	729	4.9	2.9	23	44	30	22	0.19	0.035	997
BCm	120–145	4	133	723	4.9	3.4	26	45	25	22	0.25	0.032	987
C	> 145	4	137	743	5.2	3.5	28	46	27	22	0.25	0.048	1016
VF3													
E	0–20	83	98	691	8.6	1.5	5	30	12	17	0.15	0.070	945
Bhs	20–28	163	106	558	6.9	1.4	17	33	12	45	0.20	0.079	940
Bs	28–60	78	127	642	6.5	1.9	27	40	12	32	0.19	0.055	966
BC (m)	> 60	53	120	664	6.3	1.4	3.95	43	14	35	0.28	0.067	975
VF4													
E	0–20	50	108	712	8.2	0.8	2.04	39	11	23	0.33	0.080	973
Bs1	20–38	63	117	687	8.0	0.9	1.94	36	11	30	0.41	0.092	973
Bs2	38–60	67	134	640	4.9	1.9	3.59	45	16	32	0.35	0.049	976
C	> 60	1	132	713	5.1	2.6	3.75	49	22	25	0.30	0.040	993

¹ organic matter = org.C (of the fine earth and the soil skeleton) × 1.72

Furthermore, in all soils Ti had two orders of magnitude greater concentrations and seems, thus, to be more robust. Although Ti, Zr or V might also occur as trace elements also in sheet silicates, they are considered to be almost immobile. Some investigations indicate, however, that under certain circumstances these metals may also be slightly weathered (Nieuwenhuyse and van Breemen, 1997; Cornu *et al.*, 1999). According to Table 4, the degree of chemical inhomogeneity within each single profile and also between the profiles can be considered as rather small.

Extensive mineral weathering occurs in the AE or E horizons of the soils. First, the total weight losses are compared to a standardized soil depth (0–25 cm; taking the strain into account). This has been done to enable a comparison between the clay mineral transformations and corresponding weathering processes (see below). It had to be assumed that clay mineral transformations and element losses are most advanced in the topsoil. Usually the greatest element losses are observed at the higher altitudes (Figure 3). Some of the results are in good agreement with the measurements at Val Genova. Very pronounced increases in weathering losses with altitude were observed for the elements Al and Si. The losses of Mg were much greater in Val di Fiemme than in Val Genova. The high Mg losses are probably due to the presence of more weatherable Fe-Mg phyllosilicates (Righi *et al.*, 1999; Olsson and Melkerud, 2000). For Ca, the opposite was the case. There are some inhomogeneities in the soil material that cannot be completely

ignored. The Na and Mg losses at VF2 seemed to be too low while the losses of Fe at Val Genova (at 950 m a.s.l.) were too high.

The chemical weathering of base cations (Ca, Mg, K, Na) was nearly identical at both sites (Figure 4) in the soil depth range 0–25 cm. The total amount of chemical weathering that is equivalent to the sum of losses of Al₂O₃ + SiO₂ + CaO + MgO + K₂O + Na₂O + Fe₂O₃ + MnO, however, seemed to be slightly lower in Val di Fiemme (Figure 4) if compared to Val Genova.

The elemental losses with respect to the whole soil profile gave a somewhat similar impression. The total amount of element losses (expressed as oxides) and the losses of base cations were greatest at both investigation sites, at higher altitudes. Val di Fiemme had generally slightly lower values (Table 5, Figure 5).

Clay minerals

VF1. X-ray diffraction patterns of the AE surface horizon of soil profile VF1, at 960 m a.s.l., showed a peak centered around 1.45 nm in the Mg-saturated sample (Figure 6). This peak broadened following ethylene-glycol solvation and required two elementary curves, a more intense one centered at 1.45 nm and a smaller one at 1.65 nm, for the peak-fitting procedure (Figure 7). The expanded peak indicates a low-charge mineral, while the other belongs to vermiculite, hydroxy-interlayered vermiculite (HIV) and chlorite. In fact, vermiculite collapsed to 1.0 nm after K saturation, HIV collapsed to 1.0 nm after heating at 335°C, while a small

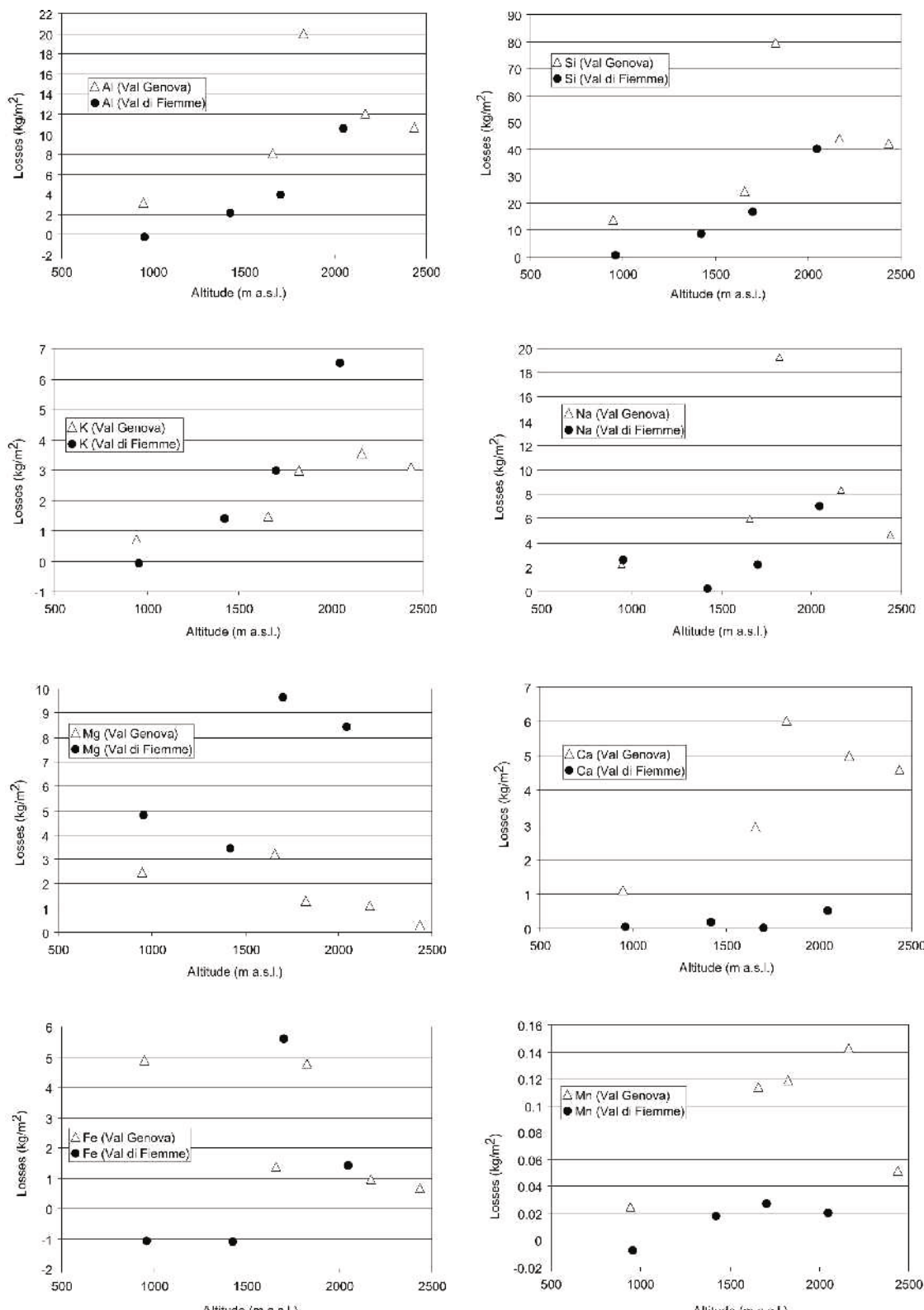


Figure 3. Weathering losses of several elements in soils as a function of the altitude at the Val di Fiemme site. These losses are standardized to the initial columnar height (25 cm) of the elementary volume (considering the strain factor, equation 3) and based on Ti as an immobile element.

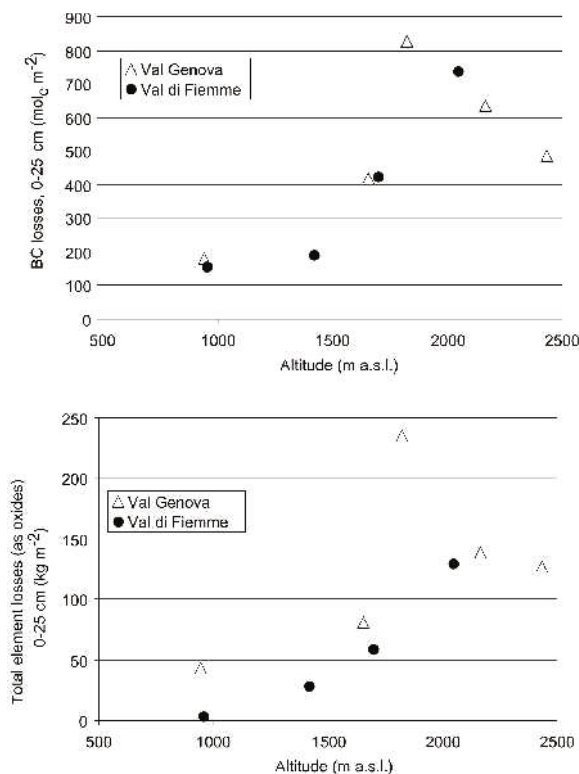


Figure 4. Base cation losses ($BC = 2Ca^{2+} + 2Mg^{2+} + K^+ + Na^+$) and chemical weathering ($= Al_2O_3 + SiO_2 + CaO + MgO + K_2O + Na_2O + Fe_2O_3 + MnO$) in soils as a function of the altitude at Val di Fiemme (and Val Genova for comparison). These losses are standardized to the initial columnar height (25 cm) of the elementary volume (considering the strain factor, equation 3) and based on Ti as an immobile element.

portion of the peak at 1.45 nm persisted in its position following the heating at 550°C (Barnhisel and Bertsch, 1989) and, thus, indicates some primary chlorite. The persistence of mineral species between 1.4 and 1.0 nm even at 550°C is due to some irregular interstratification of chlorite with HIV. Mica and kaolinite were also

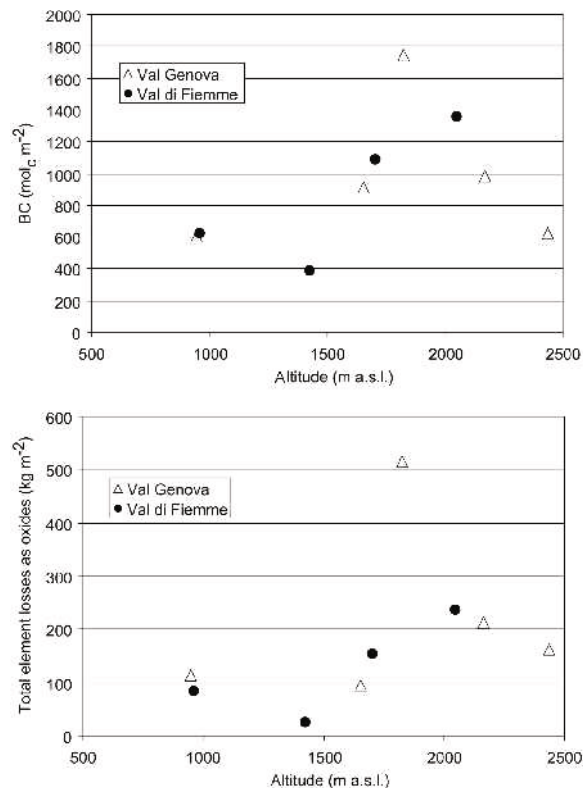


Figure 5. Base cation losses ($BC = 2Ca^{2+} + 2Mg^{2+} + K^+ + Na^+$) and chemical weathering ($= Al_2O_3 + SiO_2 + CaO + MgO + K_2O + Na_2O + Fe_2O_3 + MnO$) in soils as a function of the altitude at Val di Fiemme (and Val Genova for comparison). These losses refer to the whole soil profile and are based on Ti as an immobile element.

present, denoted by the peaks at 1.0 nm and at 0.7 nm, respectively; the latter of which disappeared following heating at 550°C. A regularly interstratified mica-2:1 clay mineral (chlorite or HIV) was characterized by the sequence of peaks at 2.34, 1.29 and 0.78 nm (Figure 7). The peak at 0.65 belongs to plagioclase.

Table 5. Weathering losses in the whole soil profiles in the investigation areas Val di Fiemme and Val Genova.

Site	Altitude (m a.s.l.)	Al (mol/ha/y)	Si (mol/ha/y)	Ca (mol/ha/y)	Mg (mol/ha/y)	K (mol/ha/y)	Na (mol/ha/y)	Fe (mol/ha/y)	Mn (mol/ha/y)
Val Genova									
	2440	336	1274	97	8	67	135	8	0.77
	2170	428	1619	133	29	87	240	11	2.54
	1830	1020	4155	212	34	108	559	57	2.96
	1660	267	495	105	88	44	174	16	3.85
	950	172	835	74	67	52	64	58	1.83
Val di Fiemme									
	VF4	2050	420	1793	16	230	204	17	0.19
	VF3	1705	234	1099	0	264	128	67	0.86
	VF2	1425	9	85	9	94	27	4	0.67
	VF1	960	49	705	5	131	67	0	0.00

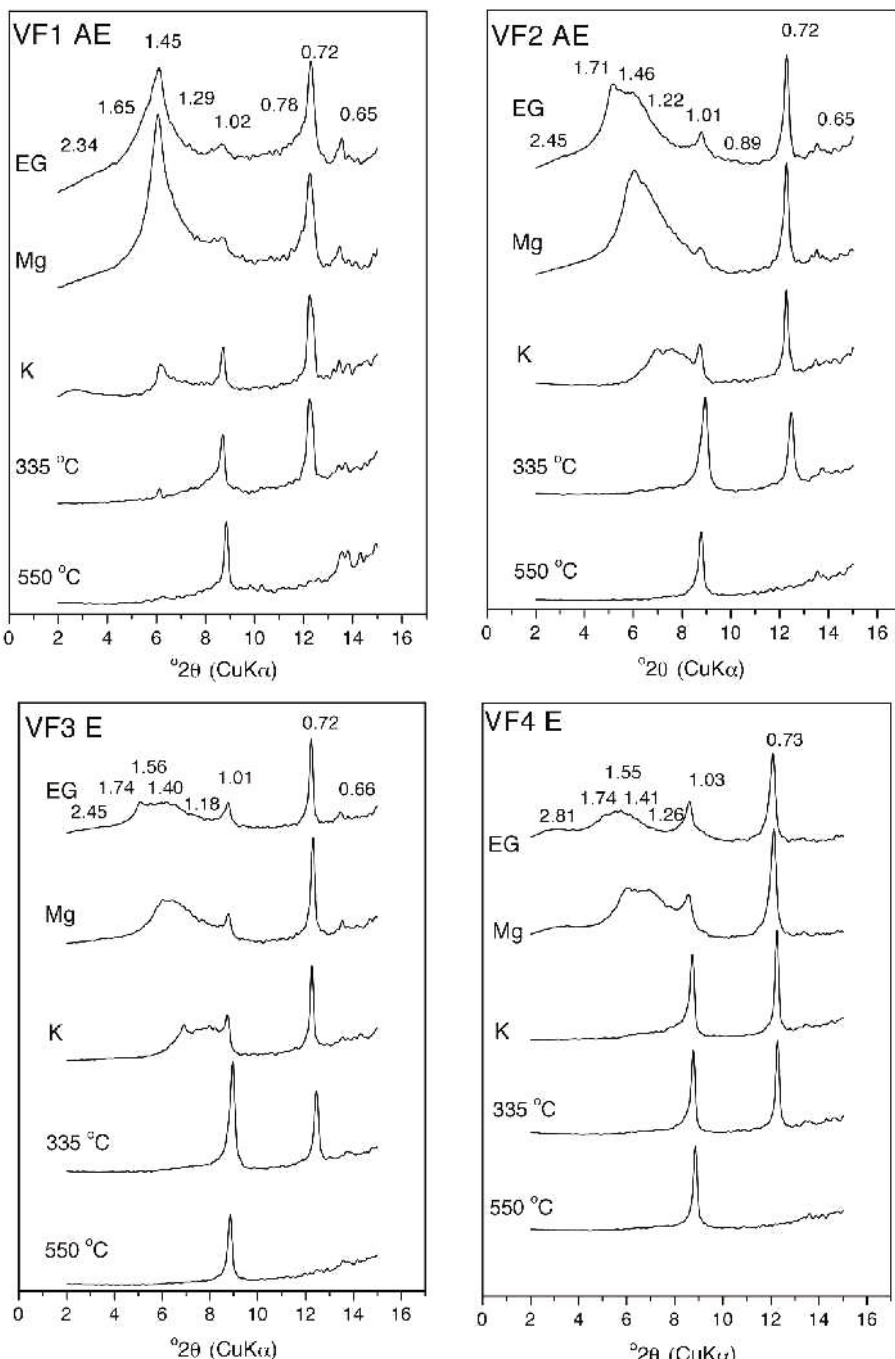


Figure 6. XRD patterns of soil clays ($<2 \mu\text{m}$) of the AE or E horizons (Val di Fiemme). The XRD curves are smoothed and corrected for Lorentz and polarization factors. d spacings are given in nm. Mg = Mg saturation, EG = ethylene glycol solvation, K = K saturation and corresponding heat treatments.

The deconvolution of the XRD pattern of the AE horizon clay sample after long-chain alkylammonium ion C18 saturation gave two pronounced elementary curves with their maximum at 4.2 and 1.80 nm (data not shown). Values of layer charges calculated from d spacings >3.1 nm are beyond the limits of the C-18 BTP regression model of Olis *et al.* (1990) and are, therefore,

indicated as >0.75 . The AE horizon is, thus, characterized by a high-charge mineral phase (with $\xi >0.75$ per half unit-cell) and a low-charge phase (with $\xi = 0.29$ per half unit-cell).

The lower Bs1 horizon was characterized by a larger amount of the HIV mineral in comparison to the vermiculite mineral. Furthermore, a small peak at

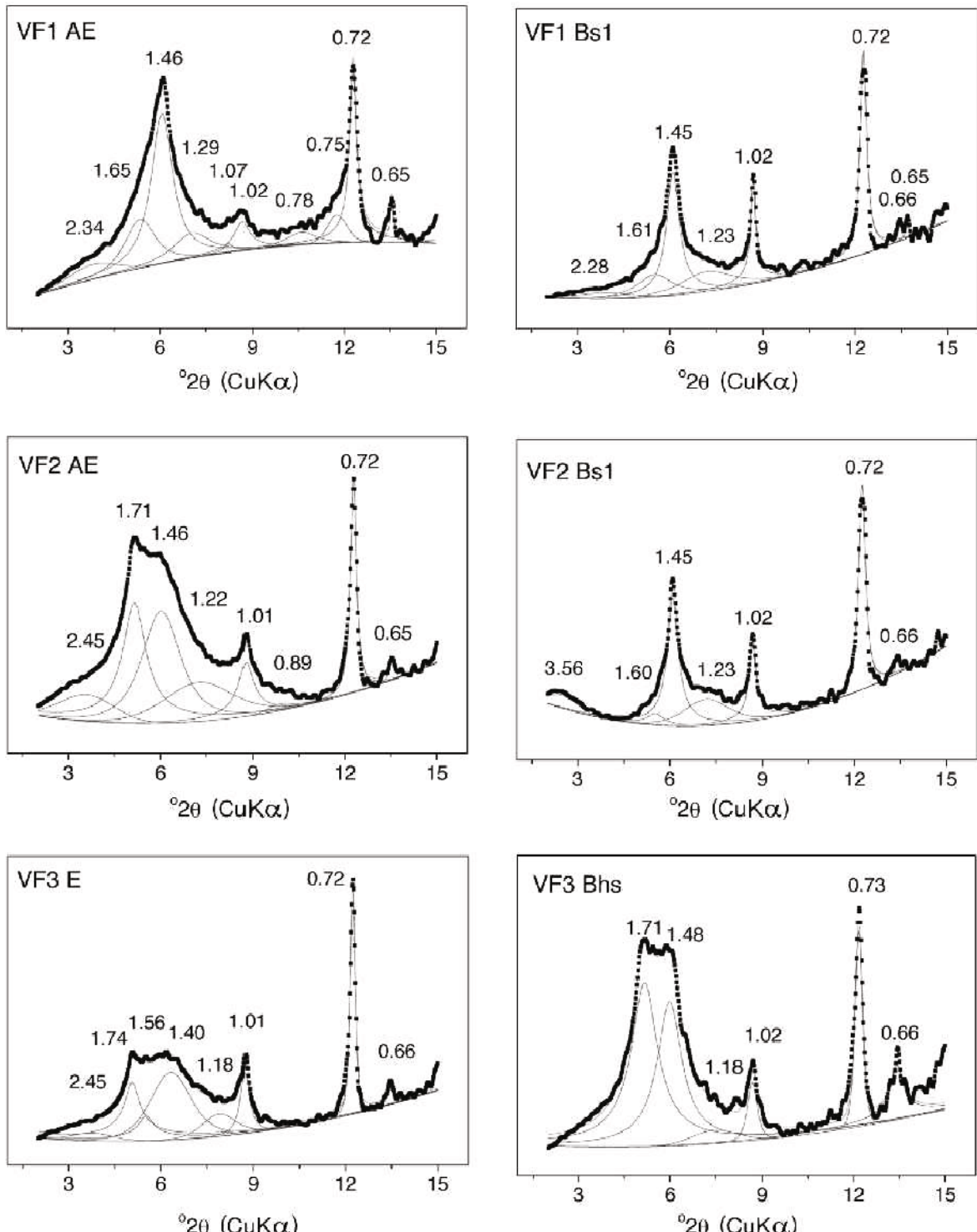


Figure 7. Peak separation of XRD patterns of ethylene-glycol solvated samples from top- and subsoils of VF1, VF2 and VF3. d spacings in nm.

1.61 nm indicated the presence of a low-charge expandable component that appears partly interstratified with a non-expandable mineral, because of the lack of expansion up to 1.65 nm. With the C-18 method, a low-charge

($\xi = 0.27$ per half unit-cell) mineral phase, one with an intermediate-charge ($\xi = 0.41$) and a high-charge component ($\xi > 0.75$) could be identified. Hydroxy-interlayered vermiculite could be detected in the Bs2

horizon, while the chlorite peak was now more evident. The C horizon showed a decrease of the intensity of the peak at 1.43 nm and a corresponding increase of the mica peak at 1.0 nm. Vermiculite and HIV were present in this sample, as indicated by the collapse of the peak at 1.43 nm to 1.0 nm, following K saturation and the heating at 335°C, respectively. Traces of some smectitic components could also be measured. Chlorite was now evident and was identified by the peak at 1.4 nm that maintained its position after heating at 550°C. The C horizon was mainly characterized by high-charge components ($\xi > 0.75$ and 0.64) and also by one with a lower charge ($\xi = 0.45$).

VF2. The XRD pattern of the Mg-saturated sample from the surface AE horizon of soil profile VF2 at 1425 m a.s.l. was characterized by a broad peak at ~1.48 nm. A relevant part of this peak expanded to 1.71 nm following EG solvation and indicating, therefore, the presence of a smectitic component with a low charge ($\xi = 0.30$). The K saturation caused a partial shift of the peak at 1.46 nm to 1.26 nm and 1.01 nm. The vermiculitic phase had a high charge ($\xi > 0.75$). Additionally, mica and kaolinite but no chlorite (no peak at 1.40 nm after heating at 550°C) could be detected.

The Bs1 and Bs2 horizons, developing below the surface AE horizon, showed similar XRD patterns. In the EG-solvated sample from the Bs1 horizon, a very small peak centered around 1.60 nm was detected (Figure 7) similar to the Bs1 horizon from the soil profile VF1. This peak represents an interstratified mineral with one of the phases consisting of a low-charge expandable mineral. The C-18 BTP model gave $\xi = 0.33$ per half unit-cell. This component was not detected in the lower Bs2 horizon. Al interlayering within the vermiculitic mineral was evident in these horizons, as indicated by the lack of collapse to 1.0 nm of the peak at 1.46 nm following K saturation.

The BCm and C horizons had more mica compared to the above horizons, as denoted by the intensity of the peak at 1.02 nm in the XRD pattern of the Mg-saturated sample. The vermiculitic component was Al-interlayered in both samples and chlorite could be identified for its peak that resisted collapse after the heat treatment at 550°C. Furthermore, an expandable mineral phase, denoted by a small peak around 1.65 nm in the EG-solvated samples, was detected in both samples. Similar to VF1, the C horizon contained high-charge components with $\xi > 0.75$ and an intermediate phase with $\xi = 0.42$.

VF3. The surface E horizon of soil profile VF3, developing at 1705 m a.s.l., showed the same types and amount of clay minerals as those detected in the AE horizon of soil profile VF2, with a similar proportion of smectitic and vermiculitic components (with charges of $\xi = 0.29$ and $\xi > 0.75$; cf. also Figure 7). The latter

maintained their 1.4 nm basal spacing after K saturation and collapsed to 1.0 nm following heating at 335°C (Figure 6). The vermiculites are, therefore, to a certain extent, Al-interlayered. The low-charge expandable mineral could also be detected in the Bhs horizon underneath, and its amount was comparable to that of the vermiculitic components. The K saturation caused a partial collapse of the 2:1 clay minerals, while an evident peak at ~1.23 nm showed that interlayers of the irregularly interstratified mica-vermiculite mineral are occupied by Al polymers. All these minerals collapsed to 1.0 nm after heating at 335°C. Therefore, no chlorite was present in the sample.

The XRD patterns of the Bs and BC horizons gave a broader peak at 1.44 nm in the Mg-saturated sample following EG solvation (Figure 7). This peak could be resolved into two components: one with a *d* spacing of 1.61 nm and the other with a *d* spacing of 1.46 nm. The first component, as in the Bs and BC horizons of the previously discussed soil profiles, represents a vermiculite-smectite interstratified mineral as confirmed by the presence of a low-charge ($\xi = 0.30$) and two higher-charged mineral phases ($\xi = 0.56$ and $\xi > 0.75$). Mica and kaolinite were also present in these horizons. Chlorite was close to the detection limit.

VF4. The EG-solvated sample from the surface E horizon of soil profile VF4, at 2050 m a.s.l., showed a broad peak around 1.5 nm in the XRD pattern. Three components could be separated with the fitting procedure, denoted by the peaks at 1.74, 1.55 and 1.41 nm (Figure 6). In the Mg-saturated sample, two components could be separated at 1.47 nm and 1.26 nm. The first component in the EG-solvated sample at 1.74 nm represents smectite, the second one at 1.55 nm, vermiculite that is irregularly interstratified with smectite, while the third component at 1.41 nm indicates the *d*₀₀₂ spacing of a regularly interstratified smectite-mica, whose position was at 1.26 nm in the Mg-saturated sample. The *d*₀₀₁ spacing of this mineral was characterized by the peaks at 2.81 and 2.45 nm in the EG-solvated and Mg-saturated samples, respectively. Smectite had a low charge ($\xi = 0.32$) and all other components a high charge with $\xi > 0.75$.

These minerals did not contain any Al polymers in the interlayer space; in fact, K saturation determined their collapse to 1.0 nm. Kaolinite was detected by the peak at 0.73 nm, which disappeared following the heat treatment at 550°C, while chlorite was absent. The basal reflections at 1.26 and 1.13 nm, respectively, in the EG-solvated and in the Mg-saturated samples, indicated an irregularly interstratified mica-smectite. Mica was denoted by an intense peak at 1.0 nm.

The EG-solvated sample of the Bs1 horizon showed a broad peak around 1.5 nm in the XRD pattern (Figure 8). Two components could be separated with the fitting procedure, denoted by the peaks at 1.66 and

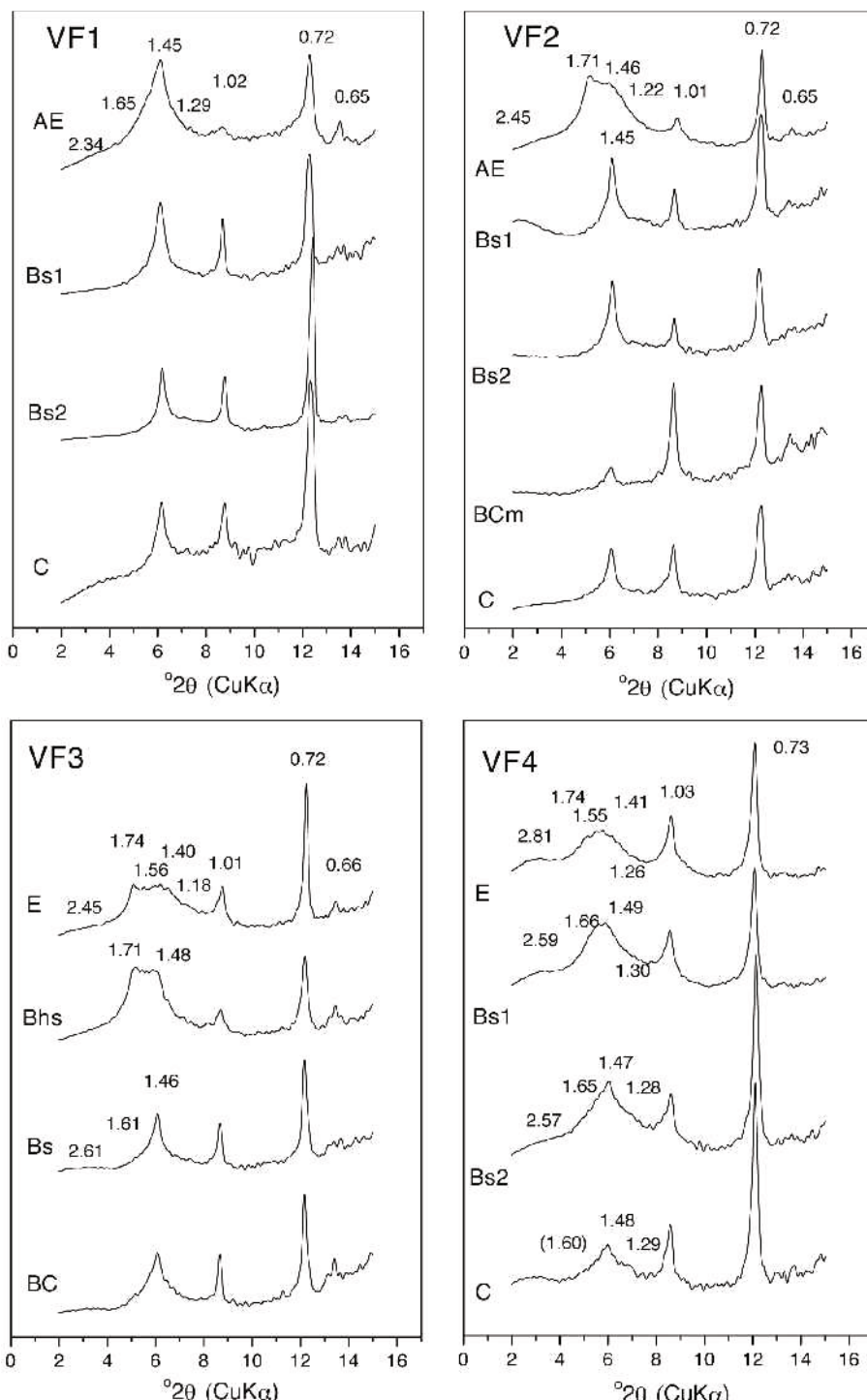


Figure 8. XRD patterns of the EG-saturated soil clays ($<2 \mu\text{m}$) of all sites (Val di Fiemme). The XRD curves are smoothed and corrected for Lorentz and polarization factors. d spacings are given in nm.

1.49 nm. These peaks were assigned to smectite and vermiculite, respectively. In fact, in the Mg-saturated sample only one peak was detected in this region centered at 1.47 nm, which collapsed to 1.0 nm following K saturation. The sequence of peaks at 2.59 and

1.30 nm in the EG-solvated sample indicated the presence of a regularly interstratified mica-vermiculite mineral. These minerals did not contain any Al polymers in the interlayer space; in fact, K saturation determined their collapse to 1.0 nm. The kaolinite peak at 0.73 nm

disappeared following the heating treatment at 550°C while chlorite was absent. The basal reflection at 1.09 nm, in the EG-solvated and in the Mg-saturated samples, indicated an irregularly interstratified mica-vermiculite. An intense peak at 1.0 nm denoted the presence of mica. Similarly to the E horizon, only low-charge ($\xi = 0.29$) and high-charge components ($\xi > 0.75$) were detectable.

Smectite was also present in the Bs2 horizon as shown by the peak at 1.65 nm in the EG-solvated sample (Figure 8). Vermiculite was characterized by the peak at 1.47 nm that partially collapsed to 1.0 nm following K saturation. The collapse to 1.0 nm was obtained after heating at 335°C. This indicates the presence of Al polymers in the interlayers of the vermiculitic component. A regularly interstratified mica-vermiculite mineral was recognized by the sequence of peaks at 2.57 and 1.28 nm in the pattern of the EG-solvated sample. An irregularly interstratified mica-vermiculite, characterized by a high proportion of mica, was also identified by the peak at 1.06 nm. The peak at 1.03 nm indicates mica, while chlorite was difficult to recognize. There was more mica present in the sample from the C horizon, than other 2:1 clay minerals. An irregularly interstratified smectite-vermiculite mineral was identified by the peak at 1.60 nm in the EG-solvated sample, that collapsed to 1.51 after Mg saturation. Vermiculite appeared to be Al-interlayered because of the lack of collapse of the peak at 1.51 nm to 1.0 nm following K saturation. The degree of Al-interlayering in the vermiculitic minerals was higher than in the samples of the over-lying horizons. An irregularly interstratified mica-Al-interlayered vermiculite mineral was identified by the peak at 1.29 nm that also maintained its position after K saturation. The presence of chlorite could now be proven by the persistence of a very small peak around 1.40 nm in the sample heated at 550°C. Also in this C horizon, phases with a variety of charges were measurable such as low-charge components ($\xi = 0.33$), intermediate phases ($\xi = 0.49$) and also high-charge minerals ($\xi = 0.5$, > 0.75).

DISCUSSION AND CONCLUSIONS

The amount of percolating water in a soil is decisive for element leaching. Although the climate is drier in Val di Fiemme, weathering losses are comparable to those of Val Genova. With respect to the clay minerals, the weathering status that is expressed by the formation of smectitic components already in the Bhs and Bs horizon and by their large amount in the surface horizons seems more advanced (Figure 8). Furthermore, a small amount of smectitic components (with a low charge, in general) was present in the parent material. There is much evidence to indicate that the smectite detected in the C horizon is derived from weathering reactions: (1) chlorite and mica, pedogenetic precursors of this

mineral (Dahlgren *et al.*, 1993; Righi *et al.*, 1993, 1999; Carnicelli *et al.*, 1997; Egli *et al.*, 2001a, 2001b, 2003), were detected in the lower horizons of the soils developing from the rhyolitic substratum. (2) The amount of smectite increases from the bottom to the surface of the soil, and correspondingly, the mica and chlorite content decreases, indicating the contribution of the pedogenetic processes to the formation of the expandable low-charge mineral (*cf.* Gillot *et al.*, 1999). (3) A better 'crystallized' smectite (or corrensite) would have been expected in the deeper horizons, indicated by a narrow peak in the XRD patterns, if this mineral had formed through a hydrothermal process. However, this was not the case in our samples.

Some mineral transformations (*i.e.* the early stages of transformation of chlorite into smectite) obviously had already occurred in the C horizon. In contrast to the study site Val di Fiemme, smectitic components were almost absent in the B and C horizons in Val Genova.

The relatively high weathering losses and the intense mineral transformation reactions in Val di Fiemme are, to a certain extent, due to the parent material that has a volcanic origin and therefore a lower degree of crystallization, although the bedrock was partially recrystallized (paleo-rhyolite). The mineralogy, the chemical composition and texture of the parent material largely determine the rate of chemical weathering, the amount of reactants distributed for synthesis of secondary materials, and the pH (Dahlgren *et al.*, 1993). There are some minor differences in texture between the two investigation sites. The parent material in Val Genova generally has a slightly higher, mean skeleton content (69% vs. 51% in Val di Fiemme). This might be an additional cause for the faster weathering processes in Val di Fiemme. In the surface horizons of the soils, these differences are, however, negligible. In contrast to the coarse material, the clay content of the fine earth in the parent material and in the soil surface horizons (Figure 9) does not differ greatly between the two investigation sites. Additionally, the amount of clays produced in the soil profile gives similar mean values (29 kg/m² for Val Genova and 30 kg/m² for Val di Fiemme), although the variation is considerably greater in Val Genova (range of values: 6–52 kg/m² vs. 23–43 kg/m² in Val di Fiemme). These calculations are based on the comparison of the clay content in the weathered profile with the parent material or least weathered horizon.

The distribution of element losses with altitude in Val di Fiemme is in agreement with the results from Val Genova. Element denudation is greatest in the subalpine forest near the timberline. Mass-balance calculations of base cations, Al, Fe and Si indicated extensive mineral weathering with relative losses (calculated according to equation 4) for Ca up to 82% (E horizon of VF4), for Mg up to 91% (E horizon of VF3) or for Al up to 48% (E-horizon, VF4). These values are close to those of mature soils reported elsewhere in the Alps (Egli *et al.*,

Table 6. Characteristics of watersheds and soil profiles on granitoid parent material and rates of element losses.

Locality	Country	Reference	Annual precipitation (mm)	Annual runoff (mm)	Mean annual temperature (°C)	Na (mol/ha/y)	K (mol/ha/y)	Ca (mol/ha/y)	Mg (mol/ha/y)	Si (mol/ha/y)
Watershed studies										
Bärhalde	GER	#	2000	1395	5+	496	324	87	98	1193
Schluchsee	GER	#	2300	1974	5+	1082	384	232	244	544
Wittenbach	GER	Schiedeck (1993)	931	408	5.5+	679	153	581	122	91
Finsterboden	GER	Pfaffenberger (1993)	1091		5.5+	100		432		
Villingen	GER	Brahmer and Feger (1989)	1638		5+	130		75	86	
Expt. Lake	CAN	#	508	225	2.4	26		5	19	
Rawson Lake E	CAN	#	803	277	2.4	121	11	87	76	544
Rawson Lake NE	CAN	#	803	277	2.4	99	34	31	50	589
Rawson Lake NW	CAN	#	803	277	2.4	48	8	21	49	387
Ciste Mheardad	GB	#	2000		5	540	128	32	144	288
Dargall	GB	#	2861	2464	6	1026	341	91	216	1489
Green Burn	GB	#	2707	2135	6	661	431	68	309	1539
White Lagan	GB	#	2822	2185	6	627	518	48	319	1004
Bhealaich	GB	Bain <i>et al.</i> (2001)				39	106		27	
Ailt a'Mharcraig	GB	Bain <i>et al.</i> (1994)	923	794	5.7	310	14	128	122	
Loch Vale	GB	Baron (1992)	1130	1310	5.8	85	25	161	44	
Birkenes	NOR	#	1637		7.5	702	7	244	96	
Bottane	NOR	#	3195		7.5	479	11	176	160	
Kaarvatn	NOR	#	2252	1899	5.2	230	144	19	30	
Sogndal	NOR	#	984	875		29		54	6	130
Storgama	NOR	#	1192	923	7.1	122	119		33	
Hartviko	Cz	#	781	467	6	139	23		21	507
Salacova Lhota	Cz	#	685	128	6.5	138	10	45	85	542
Vocadio	Cz	#	736	171	6.5	377	64	498	293	535
Däntersta	SWE	#	610	115	0.3	204	33	177	182	
Lilla Tivsjön	SWE	#	623	203	2	59		200	106	
Solmyren	SWE	#	621	348	0.3	128	30	315	138	
Vuoddasbäcken	SWE	#	621	383	0.3	171	14	177	110	
Bear Brook	USA	#	1400	881	5	184	61	361	124	485
Cadwell Creek	USA	#	831	793	7	223		217	89	849
Log Creek	USA	#	887	363	7.2	382	52	281	56	466
Panther Lake	USA	#	1170	720	5	204	147	574	147	
Rabbit Ears	USA	#	1132	617	0.7	236	44	186	114	659
Tarps Creek	USA	#	887	187	7.2	92	3		15	425
Tesque Aspin	USA	#	946	639	5	647	74	307	217	
Tesque Conifer	USA	#	1149	829	2.5	567	91	396	176	
Woods Lake	USA	#	1230	760	5	25	83		14	
Hubbard Brook	USA	Likens <i>et al.</i> (1977)	1300	490	6	244	26	287	103	847

Bhealaich 3	GB	Bain <i>et al.</i> (2001)						
Bhealaich 4	GB	Bain <i>et al.</i> (2001)						
Ailt 'a'Mharcaidh*	GB	Bain <i>et al.</i> (1994)						
Ailt 'a'Mharcaidh**	GB	Bain <i>et al.</i> (1994)						
Nyänget	SWE	Olsson and Melkerud (2000)	923	794	5.7	102	3	0
Heden	SWE	Olsson and Melkerud (2000)	923	794	5.7	107	12	2
Hyttfältä	FINL	Olsson and Melkerud (2000)	923	794	5.7	72	12	14
Schmaderi	CH	Egli <i>et al.</i> (2001)	2000	2000	1.4	77	9	17
Gletsch	CH	Egli <i>et al.</i> (2001)	2000	2000	1.4	42	38	25
						117	61	39
						118	62	36
						274	223	40
						326	155	25
							119	119
							2451	2451
							1981	1981

Detailed references of the sites are listed in White and Blum (1995). Only sites with a mean annual temperature of <8°C were selected from the list given in White and Blum (1995)

* Alpine Podzols

** Peaty Podzols

+ estimated

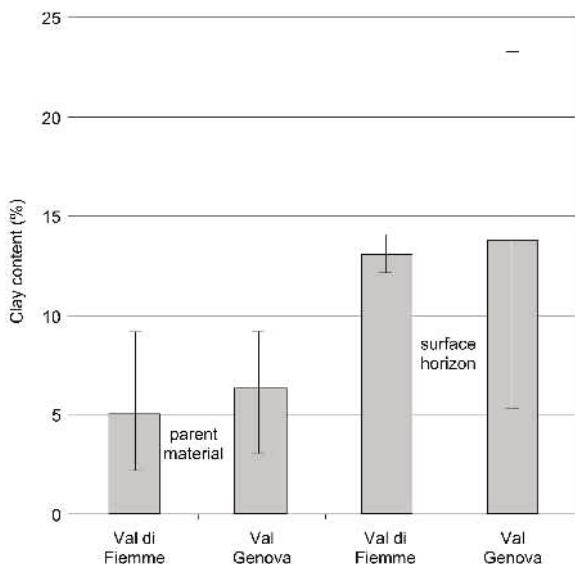


Figure 9. Mean values of the clay content in the surface horizon and in the parent material of the Val di Fiemme and Val Genova sites.

2001b). There are, however, differences between the two sites with respect to absolute losses of single elements such as Ca, K or Mg, which are caused by a different mineralogy of the parent material. The Ca content in the samples of Val di Fiemme was one order of magnitude lower than in Val Genova while the K content is twice that of Val Genova. The K-feldspar content in Val di Fiemme was higher and consequently also the corresponding weathering losses. The measured losses of Na, Ca, K, Mg and Si (Table 5 and Figure 5) in Val di Fiemme and Val Genova correspond well with values reported from watershed and profile studies presented in Table 6. Weathering rates vary greatly due to the different climates, differences in the parent material and, especially with regard to watershed studies, due to different loads of acidity. For some soils in the climosequence (Val die Fiemme and Val Genova), silicon losses seemed to be particularly high (similar to some sites in the Swiss Alps) highlighting the intense weathering processes in the subalpine to alpine climate range.

Kaolinite in the clay fraction can presumably be traced back to the weathering of plagioclase, although Ross (1980) pointed out how this is in apparent disagreement with thermodynamic equilibrium calculations. He endorsed the view that this contrast is due to incomplete evolution and the non-equilibrium of soils that, in most cases, are geologically young and develop in rather cool climates. Due to the higher plagioclase content in Val Genova, the corresponding kaolinite content was also slightly higher (9% vs. 6% in Val di Fiemme). Kaolinite is generally found as a minor constituent in young soils, and by implication is considered to require >10,000 y to form (Wilson, 1999). It may be an abundant constituent of soils

developed upon old geomorphic surfaces. Similar to Val Genova, the largest amount of smectitic components in Val di Fiemme was measured in the subalpine forest (Figure 10). The pattern of smectite distribution along the climosequence followed the trend of weathering losses of base cations, Al and Si. The presence of smectite is, therefore, bound to strong leaching and weathering conditions (*cf.* Righi *et al.*, 1999). The formation of smectite is due to the transformation of chlorite and mica (over transitional steps such as irregularly interstratified mica-vermiculite or vermiculite-smectite). In contrast to that, the trend of the sum of chlorite + HIV is opposite with a minimum near the timberline and a higher value at lower or higher altitudes. These new results support the hypothesis of Egli *et al.* (2003) that there is a pronounced 'podzolization' effect in subalpine forest near the timberline; this means that weathering is greater in this region than in montane environments or in alpine tundra. This fact seems to be due to a combined effect of temperature and precipitation, vegetation (and the corresponding release of organic ligands) and dissolution kinetics of minerals (Egli *et al.*, 2003).

The soil water fluxes are increasing in the Alps with altitude due to higher precipitation and decreasing temperatures. Net export of elements may thus also be higher with increasing altitudes.

The stemflow as well as the litter of coniferous trees lead to an intensified acidification of the soil (*cf.* Certini *et al.*, 1998) and to a higher production of organic ligands in the soil water. These conditions promote the appearance of a low-charge expandable mineral (smectite). Smectites are formed from chlorite through removal of hydroxy-interlayers and reduction of layer charge, the extraction of the interlayer polymers being enhanced by organic complexing agents (Carnicelli *et al.*, 1997; Castaldini *et al.*, 2002). Higher concentrations of organic ligands in the soil solution may generally lead

to enhanced weathering rates (Stumm and Wieland, 1990).

Dissolution kinetics of minerals are often temperature dependent (Stumm and Morgan, 1996). Usually, the lower the temperature (and consequently the higher the altitude), the lower the weathering rate.

ACKNOWLEDGMENTS

We would like to express our appreciation to B. Kägi and D. Giacca for the laboratory work. We are, furthermore, indebted to Dr M.-L. Räsänen and an unknown reviewer for their helpful comments on an earlier version of the manuscript.

REFERENCES

- Bain, D.C., Mellor, A., Wilson, M.J. and Duthie, D.M.L. (1994) Chemical and mineralogical weathering rates and processes in an upland granitic till catchment in Scotland. *Water, Air, and Soil Pollution*, **73**, 11–27.
- Bain, D.C., Roe, M.J., Duthie, D.M.L. and Thomson, C.M. (2001) The influence of mineralogy on weathering rates and processes in an acid-sensitive granitic catchment. *Applied Geochemistry*, **16**, 931–937.
- Barnhisel, R.I. and Bertsch, P.M. (1989) Chlorites and hydroxy-interlayered vermiculite and smectite. Pp. 729–788: in *Minerals in Soil Environments*, 2nd edition (J.B. Dixon and S.B. Weed, editors). Soil Science Society of America, Madison, Wisconsin.
- Baron, J. (1992) *Biogeochemistry of a Subalpine Ecosystem*. Springer-Verlag, New York.
- Berner, R.A. and Lasaga, A.C. (1989) Modeling the Geochemical Carbon Cycle. *Scientific American*, **260**, 74–81.
- Bockheim, J.G., Munroe, J.S., Douglass, D. and Koerner, D. (2000) Soil development along an elevational gradient in the southeastern Uinta Mountains, Utah, USA. *Catena*, **39**, 169–185.
- Brahmer, G. and Feger, K.-H. (1989) Hydrochemische Bilanzen kleiner bewaldeter Einzugsgebiete des Südschwarzwaldes. Pp. 205–211 in: *Immissionsbelastung des Waldes und seiner Böden – Gefahr für die Gewässer?* (H. Brechtel, editor). DVWK Mitteilungen 17, Bonn, Germany.
- Brimhall, G.H. and Dietrich, W.E. (1987) Constitutive mass balance relations between chemical composition, volume, density, porosity, and strain in metasomatic hydrochemical systems: Results on weathering and pedogenesis. *Geochimica et Cosmochimica Acta*, **51**, 567–587.
- Carnicelli, S., Mirabella, A., Cecchini, G. and Sanesi, G. (1997) Weathering of chlorite to a low-charge expandable mineral in a spodosol on the Apennine mountains, Italy. *Clays and Clay Minerals*, **45**, 28–41.
- Castaldini, M., Egli, M., Mirabella, A., Fabiani, A., Santomassimo, F. and Miclaus, N. (2002) Influence of climate on soil development and microbial community in Trentino mountains – Italy. *BGS Bulletin*, **25**, 55–60.
- Certini, G., Ugolini, F.C., Corti, G. and Agnelli, A. (1998) Early stages of podzolization under Corsican pine (*Pinus nigra* Arn. ssp. *laricio*). *Geoderma*, **83**, 103–125.
- Chadwick, O.A., Brimhall, G.H. and Hendricks, D.M. (1990) From a black to a gray box – a mass balance interpretation of pedogenesis. *Geomorphology*, **3**, 369–390.
- Cornu, S., Lucas, Y., Lebon, E., Ambrosi, J.P., Luziao, F., Rouiller, J., Bonnay, M. and Neal, C. (1999) Evidence of titanium mobility in soil profiles, Manaus, central Amazonia. *Geoderma*, **91**, 281–295.

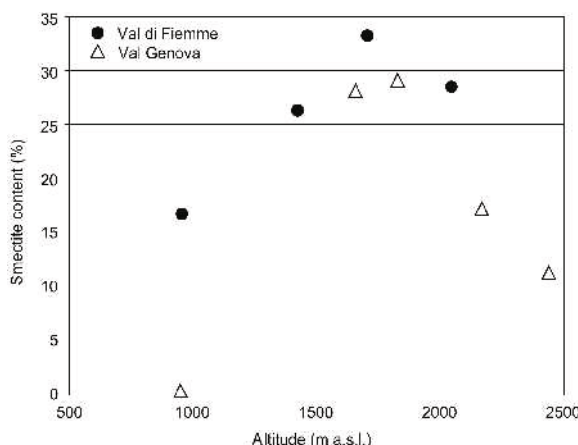


Figure 10. Relationship between the smectite content in the most weathered horizons (surface horizons) of Val di Fiemme (and Val Genova for comparison) and the altitude.

- Costantini, E., Mancabelli, A., Sartori, G., Wolf, U., Falcetti, M., De Ros, G., Tonon, C., Mescalchin, E. and Pinzauti, S. (1995) *Per le vigne e i boschi del Trentino. Lo studio dei suoli applicato alla zona viticola e alla gestione degli ecosistemi forestali*. Guida all'escurzione, Associazione Italiana Pedologi, San Michele all'Adige.
- Dahlgren, R., Shoji, S. and Nanzyo, M. (1993) Mineralogical characteristics of volcanic ash soils. Pp. 101–143 in: *Ash Soils, Genesis, Properties and Utilization* (S. Shoji, M. Nanzyo and R. Dahlgren, editors). Developments in Soil Science, **21**. Elsevier Science Publishers B.V., Amsterdam, The Netherlands.
- Egli, M. and Fitze, P. (2000) Formulation of pedologic mass balance based on immobile elements: a revision. *Soil Science*, **165**, 437–443.
- Egli, M., Mirabella, A. and Fitze, P. (2001a) Clay mineral formation in soils of two different chronosequences in the Swiss Alps. *Geoderma*, **104**, 145–175.
- Egli, M., Fitze, P. and Mirabella, A. (2001b) Weathering and evolution of soils formed on granitic, glacial deposits: results from chronosequences of Swiss alpine environments. *Catena*, **45**, 19–47.
- Egli, M., Mirabella, A., Sartori, G. and Fitze, P. (2003) Weathering rates as a function of climate: results from a climosequence of the Val Genova (Trentino, Italian Alps). *Geoderma*, **111**, 99–121.
- Fitze, P., Kägi, B. and Egli, M. (2000) *Laboranleitung zur Untersuchung von Boden und Wasser*. Geographisches Institut der Universität Zürich, Zürich, Switzerland.
- Gillot, F., Righi, D. and Räsänen, M.L. (1999) Formation of smectites and their alteration in two chronosequences of podzols in Finland. Pp. 725–731 in: *Clays for our Future* (H. Kodama, H.R. Mermut and J.K. Torrace, editors). 11th International Clay Conference 1997, ICC97, Ottawa, Canada.
- Gustafsson, J.P., Bhattacharya, P., Bain, D.C., Fraser, A.R. and McHardy, W.J. (1995) Podzolisation mechanisms and the synthesis of imogolite in northern Scandinavia. *Geoderma*, **66**, 167–184.
- Hitz, C., Egli, M. and Fitze, P. (2002) Determination of the sampling volume for representative analysis of alpine soils. *Zeitschrift für Pflanzenernährung und Bodenkunde*, **165**, 326–331.
- Jenny, H. (1980) *The Soil Resource*. Springer, New York.
- Lanson, B. (1997) Decomposition of experimental X-ray diffraction patterns (profile fitting): a convenient way to study clay minerals. *Clays and Clay Minerals*, **45**, 132–146.
- Likens, G.E., Bormann, F.H., Pierce, R.S., Eaton, J.S. and Johnson, N.M. (1977) *Biogeochemistry of a Forested Ecosystem*. Springer-Verlag, New York.
- Lumsdon, D.G. and Farmer, V.C. (1997) Solubility of a proto-imogolite sol in oxalate solutions. *European Journal of Soil Science*, **48**, 115–120.
- Mahaney, W.C. (1978) Late-Quaternary stratigraphy and soils in the Wind River Mountains, western Wyoming. Pp. 223–264 in: *Quaternary Soils* (W.C. Mahaney, editor). Geo-Abstracts, Norwich, UK.
- McKeague, J.A., Brydon, J.E. and Miles, N.M. (1971) Differentiation of forms of extractable iron and aluminium in soils. *Soil Science Society of America Proceedings*, **35**, 33–38.
- Mirabella, A. and Sartori, G. (1998) The effect of climate on the mineralogical properties of soils from the Val Genova Valley (Trentino, Italy). *Fresenius Environmental Bulletin*, **7**, 478–483.
- Mirabella, A., Egli, M., Carnicelli, S. and Sartori, G. (2002) Influence of parent material on clay minerals formation in podzols of Trentino, Italy. *Clay Minerals*, **37**, 699–707.
- Moore, D.M. and Reynolds, R.C. (1997) *X-ray diffraction and the Identification and Analysis of Clay Minerals*, 2nd edition. Oxford University Press, New York.
- Nieuwenhuysse, A. and van Breemen, N. (1997) Quantitative aspects of weathering and neof ormation in selected Costa Rican volcanic soils. *Journal of the Soil Science Society of America*, **61**, 1450–1458.
- Olis, A.C., Malla, P.B. and Douglas, L.A. (1990) The rapid estimation of the layer charges of 2:1 expanding clays from a single alkylammonium ion expansion. *Clay Minerals*, **25**, 39–50.
- Olsson, M.T. and Melkerud P.-A. (2000) Weathering in three podzolized pedons on glacial deposits in northern Sweden and central Finland. *Geoderma*, **94**, 149–161.
- Parfitt, R.L. and Hemmi, T. (1982) Comparison of an oxalate-extraction method and an infrared spectroscopic method for determining allophane in soil clays. *Soil Science and Plant Nutrition*, **28**, 183–190.
- Pfaffenberger, C. (1993) Stoffaustrag in einem Buntsandstein-Gebiet (Finsterboden). Pp. 157–161 in: *Eintiefungsgeschichte und Stoffaustrag im Wutachgebiet (SW-Deutschland)* (G. Einsele and W. Ricken, editors). Tübinger geowissenschaftliche Arbeiten, Reihe C 15, Tübingen, Germany.
- Righi, D. and Meunier, A. (1991) Characterization and genetic interpretation of clays in acid brown soil (Dystrochrept) developed in a granitic saprolite. *Clays and Clay Minerals*, **39**, 519–530.
- Righi, D., Petit, S. and Bouchet, A. (1993) Characterization of hydroxy-interlayered vermiculite and illite/smectite interstratified minerals from the weathering of chlorite in a Cryorthod. *Clays and Clay Minerals*, **41**, 484–495.
- Righi, D., Huber, K. and Keller, C. (1999) Clay formation and podzol development from postglacial moraines in Switzerland. *Clay Minerals*, **34**, 319–332.
- Ross, G.J. (1980) The mineralogy of Spodosols. Pp. 127–143 in: *Soils with Variable Charge* (B.K.G. Theng, editor). Soil Bureau, Department of Scientific and Industrial Research, Lower Hutt, New Zealand.
- Schiedeck, T. (1993) Stoffaustrag in einem bewaldeten Granit-Einzugsgebiet (Wittenbach). Pp. 149–156 in: *Eintiefungsgeschichte und Stoffaustrag im Wutachgebiet (SW Deutschland)* (G. Einsele and W. Ricken, editors). Tübinger geowissenschaftliche Arbeiten, Reihe C 15, Tübingen, Germany.
- Servizio Idrografico (1959) *Precipitazione media mensili ed annue per il Trentino 1921–1950*. Istituto Poligrafico dello Stato, Rome.
- Stumm, W. and Morgan, J.J. (1996) *Aquatic Chemistry*, 3rd edition. John Wiley & Sons, Inc., New York.
- Stumm, W. and Wieland, E. (1990) Dissolution of oxide and silicate minerals: rates depend on surface speciation. Pp. 367–398 in: *Aquatic Chemical Kinetics: Reaction Rates of Processes in Natural Waters* (W. Stumm, editor). Wiley-Interscience, New York.
- White, A.F. and Blum, A.E. (1995) Effects of climate on chemical weathering in watersheds. *Geochimica et Cosmochimica Acta*, **59**, 1729–1747.
- Whittaker, R.H., Buol, S.W., Niering, W.A. and Havens, Y.H. (1968) A soil and vegetation pattern in the Santa Catalina Mountains, Arizona. *Soil Science*, **105**, 440–450.
- Wilson, M.J. (1999) The origin and formation of clay minerals in soils: past, present and future perspectives. *Clay Minerals*, **34**, 7–25.
- WRB (1998) *World Reference Base for Soil Resources*. World Soil Resources Reports 84, FAO, Rome.

(Received 23 June 2003; revised 24 November 2003; Ms. 811)